Available online at www.sciencedirect.com

ScienceDirect

IFAC PapersOnline CONFERENCE PAPER ARCHIVE

IFAC PapersOnLine 58-30 (2024) 272–277

Validation of Human-Variability Respecting Optimal Control: A Preparational Study

Sean Kille, Leon Sobeloff, Sebastian Andreas Fritz, Balint Varga, Sören Hohmann

Institute of Control Systems, Karlsruhe Institute of Technology, 76131 Karlsruhe, Germany (e-mail: sean.kille@kit.edu).

Abstract: In order to design a performant and especially well perceived automation to assist the human in physical Human-Machine Interaction, an understanding of the human natural behavior is crucial. Model-based control design is therefore a favorable solution, already being used in various applications. However, most approaches model the human to be deterministic in it's behavior, not aligning to the state-of-the-art models presented by neuroscience, which more accurately describe the human to be under the influence of noise processes. This paper presents a study that examines 13 participants performing point-to-point movements, followed by the identification of the underlaying cost as well as additive and multiplicative noise process parameters of a human stochastic model. The gained results provide a basis for future automations that explicitly incorporate human variability in their control design.

Keywords: Design Methodology for HMS, Inverse Stochastic Optimal Control, Human Centred Automation, Stochastic System Identification, Cooperative Control

1. INTRODUCTION

Physical Human-Machine Interaction describes the haptically coupled action of a human and a robot, jointly acting upon a system. Teaming these two agents allows for a gainful combination of each other's strenghts, which results in potential applications in various domains. Common examples are found where repetitive and/or physical work is performed in unstructured environments, allowing to combine the robots physical strength and precision with the human flexibility to adapt. Exemplary cases are shown in collaborative welding (Wang et al. (2019)), collaborative manufacturing (Guerin et al. (2014)), and physicial assistance of human walking movements (Schneider et al. (2022)). Shared control deals with the control of such an automation, aiming at providing a performant and intuitive interaction (Abbink et al. (2012)). The resulting behavior strongly depends on the automation's parametrization, for which different approaches exist: A straightforward advance is to heuristically tune the parameters for the desired behavior (e.g. Mulder et al. (2012)), however, being tedious and task-specific. More elaborate approaches are model-based, relying on an abstraction of the human behavior: One approach is to model the human as an impedance system and shape the overall impedance as desired (e.g. Ficuciello et al. (2015), Dong et al. (2020)), resutling in improved performance but usually missing an active support. Latest methods describe human behavior using optimality principles, modeling the interaction using a dynamic game (e.g. Varga (2024), Franceschi et al. (2023)), leading to a generalizable approach to design an automation.

Most currently used model-based shared control approaches assume that the human behaves deterministically. However, neurosocientific literature shows that the human acts stochastically (Abend et al. (1982), Harris and Wolpert (1998)) and focuses on a successful task completion only in areas that are relevant for the task at hand. This results in a focus of precision in task-relevant areas, and an unstructured, high variability, execution in task-irrelevant areas. This observation is termed minimal intervention principle (Todorov and Jordan (2002)). This stochastic behavior can most-suitably be modeled using stochastic optimal control models (Todorov (2005)), the most common representative being a linear-quadratic sensorimotor (LQS) model. Knowledge of this stochasticity and it's modeling opens up the opportunity to design more human-centric control concepts which explicitly incorporate the human variability in the controller design. The expected benefits are an increased task performance and a potentially improved experience, as presented in simulation in our previous work Kille et al. (2024). A prerequisite for this novel concept is the knownledge of human behavior, meaning that the LQS model parameters that model an individual's movement behavior, need to be identified.

This paper deals with the first practical step towards such a variability-respecting control design. It presents an identification of human point-to-point reaching movements as a LQS model, including the observed variability patterns. On this basis, further work can then use the gained insights to aid in the design of novel control concepts that explicitly consider human inherent variability. This work firstly presents the system configuration which allows a human to haptically interact with a simulated system using a robotic arm. The experimental setup is kept highly modular, allowing it to be transferred to real-world systems and be supplemented with an automation resulting in a beneficial human-machine interaction. We then introduce the LQS

10.1016/j.ifacol.2025.01.193

model for goal-directed human movements. Furthermore, a subject study is conducted, in which 13 subjects move a simulated point-mass using a goal-directed movement. We analyze the movements and identify the matching parameters of the LQS model using inverse stochastic optimal control, allowing us to gain an understanding on the average human behavior and it's variability resulting through noise processes. This identification is crucial for further works, which will then be able to parametrize controllers that are personalized to individual subjects and allow the consideration of individual variability patterns.

2. MATERIALS AND METHODS

In the following section, we firstly display related works from which this paper distinguishes. Subsequently, we present 1) the system configuration, 2) the to-be-identified human stochastic optimal control model, and 3) the identification procedure.

2.1 Related works

With the awareness that human movements can be described using optimality principles, the identification of this behavior, i.e. the estimation of model parameters that result in a simulated behavior that matches the human behavior, has been of large interest.

The identification of human arm movements using inverse optimal control has been applied in various cases, the first works being by e.g. Liu et al. (2005) which minimize the joint torque within the objective function. A surge of research leads to various adaptions and extensions, e.g. Panchea et al. (2018) using a combination of multiple objective functions. Inverse optimal control methods have been applied to point-to-point movements (Berret et al. (2011)), reaching tasks in manufacturing (Sylla et al. (2014)) or locomotion trajectories (Mombaur et al. (2010)). In recent years, an extension to the two-player case using differential games has sparked interest (Rothfuß et al. (2017)). However, all these approaches identify the human as a deterministic player. Only few proposals exist which deal with the identification of a stochastic human. Chen and Ziebart (2015) and Priess et al. (2014) show first attempts at identifying the linear-quadratic gaussian case including additive noise, but neglecting multiplicative noise. With Karg et al. (2024) a computationally efficient approach which allows the identification of the additive and multiplicative noise processes is introduced and a similar previous version has been validated on identifying human driving behavior in Karg et al. (2023). An application to reaching movements as well as further using the noise parameters as a basis for controller parametrization is still outstanding. This paper deals with the former, aiming to therewith provide a basis for future controller designs.

2.2 System configuration

In order to analyze physical Human-Robot Interaction, we implement an experimental setup that allows for haptic interaction in which a human, and optionally an automation, manipulate a simulated system. As a haptic interface we include a robotic arm (KUKA LBR iiwa 14 R820) using the control concepts as introduced by Braun et al. (2023). In the presented configuration it features a large quadratic workspace of 320 x 320 mm and allows for the measuring and exertion of forces and torques.

As a communication framework we choose the robot operating system (ROS) (Quigley et al. (2009)), allowing us to implement each software component as a seperate element. The interplay of all components of the overall system structure is depicted in Fig. 1.

Both an automation and a human can manipulate a virtual system, e.g. a simulated point-mass, through their input $\boldsymbol{u}_\mathrm{A}$ and $\boldsymbol{u}_\mathrm{H}$. We describe the time-discrete linear system dynamics with

$$\begin{aligned}\boldsymbol{x}_{t+1} =& \boldsymbol{A}\boldsymbol{x}_t + \boldsymbol{B}_\mathrm{A}\boldsymbol{u}_{\mathrm{A},t} + \boldsymbol{B}_\mathrm{H}\boldsymbol{u}_{\mathrm{H},t} \\ &+ \boldsymbol{\Sigma}^{\boldsymbol{\alpha}}\boldsymbol{\alpha}_t + \sum_i^c \boldsymbol{\sigma}_i^{\boldsymbol{u}}\varepsilon_t^{(i)}\boldsymbol{B}_\mathrm{H}\boldsymbol{F}_i\boldsymbol{u}_{\mathrm{H},t}, \end{aligned} \tag{1}$$

$$\boldsymbol{y}_{\mathrm{H},t} = \boldsymbol{H}_\mathrm{H}\boldsymbol{x}_t + \boldsymbol{\Sigma}^{\boldsymbol{\beta}}\boldsymbol{\beta}_t + \sum_i^d \boldsymbol{\sigma}_i^{\boldsymbol{x}}\epsilon_t^{(i)}\boldsymbol{H}_\mathrm{H}\boldsymbol{G}_i\boldsymbol{x}_t, \tag{2}$$

where $\boldsymbol{x} \in \mathbb{R}^n$ denotes the system state, $\boldsymbol{u}_\mathrm{H} \in \mathbb{R}^{m_H}$ and $\boldsymbol{u}_\mathrm{A} \in \mathbb{R}^{m_A}$ the control variables of the human and automation, respectively, and $\boldsymbol{y}_\mathrm{H}$ the human perception. In the human action we encounter an additive standard white Gaussian noise process $\boldsymbol{\alpha}_t$ with scaling parameters $\boldsymbol{\Sigma}^{\boldsymbol{\alpha}} \in \mathbb{R}^n$ and a control-dependent noise process $\sum_i^c \boldsymbol{\sigma}_i^{\boldsymbol{u}}\varepsilon_t^{(i)}\boldsymbol{B}\boldsymbol{F}_i\boldsymbol{u}_{\mathrm{H},t}$. The human perception is overlayed with an additive standard white Gaussian noise $\boldsymbol{\beta}_t$ and scaling parameters $\boldsymbol{\Sigma}_t^{\boldsymbol{\beta}}$ as well as the multiplicative noise process $\sum_i^d \boldsymbol{\sigma}_i^{\boldsymbol{x}}\epsilon_t^{(i)}\boldsymbol{H}\boldsymbol{G}_i\boldsymbol{x}_t$ with $\boldsymbol{\epsilon} = \left[\epsilon_t^{(1)} \dots \epsilon_t^{(d)}\right]^\intercal$ denoting a standard white Gaussian noise. The multiplicative noise processes are scaled with the constants $\boldsymbol{\sigma}_i^{\boldsymbol{u}}$ and $\boldsymbol{\sigma}_i^{\boldsymbol{x}}$.

With $\boldsymbol{A}, \boldsymbol{B}_\mathrm{A}, \boldsymbol{B}_\mathrm{H}, \boldsymbol{\Sigma}^{\boldsymbol{\alpha}}, \boldsymbol{F}_i, \boldsymbol{H}_\mathrm{H}, \boldsymbol{\Sigma}^{\boldsymbol{\beta}}, \boldsymbol{G}_i$ we introduce matrices of appropriate dimension and $\boldsymbol{\varepsilon} = \left[\varepsilon_t^{(1)} \dots \varepsilon_t^{(c)}\right]^\intercal$ denotes a standard white Gaussion noise process. The stochastic process $\boldsymbol{x}_t$ is initialized with $\mathrm{E}\{\boldsymbol{x}_0\}$ and $\mathrm{cov}(\boldsymbol{x}_0, \boldsymbol{x}_0) = \boldsymbol{\Omega}_0^{\boldsymbol{x}}$.

The human's input of force $\boldsymbol{f}_\mathrm{H}$ is measured via the robot's torque sensors which are transformed to cartesian forces. The virtual system's position state $\boldsymbol{p}$ is communicated to the robot as a set-point, which results in a feedback-loop that allows the human to receive haptic feedback of the system state. A graphical user interface additionally visually displays the system's current position $\boldsymbol{p}$ and the reference points $\boldsymbol{T}_i$, see Fig. 2.

2.3 Stochastic Optimal Control Model for Goal-Directed Human Movements

We model the human movement using a LQS model for goal-directed movements as introduced by Todorov (2005), resulting in the state equation (1) with $\boldsymbol{u}_\mathrm{A} = \boldsymbol{0}$.

According to the LQS model, the human control law aims at minimizing the performance criterion

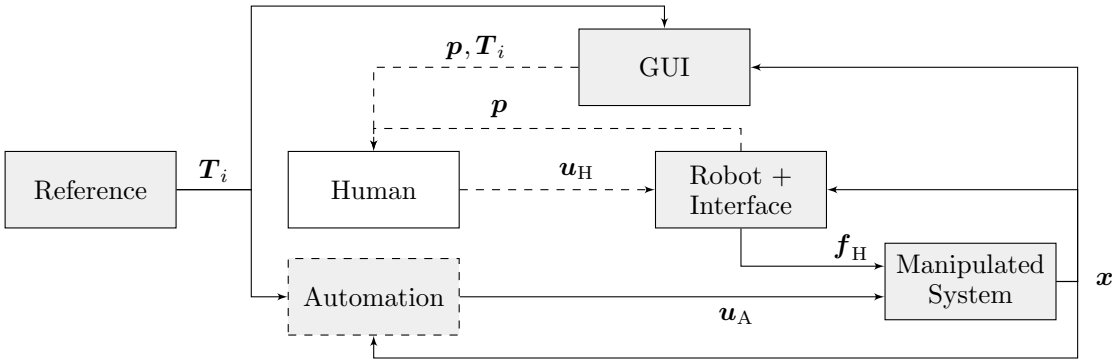

Fig. 1. Overview of the software components and the interacting human. ROS nodes are visualized in grey. The automation was set to $\boldsymbol{u}_\mathrm{A} = \boldsymbol{0}$ in this work. ROS topics are represented with solid arrows. Human's visual perception and haptic interaction is represented with dashed arrows.

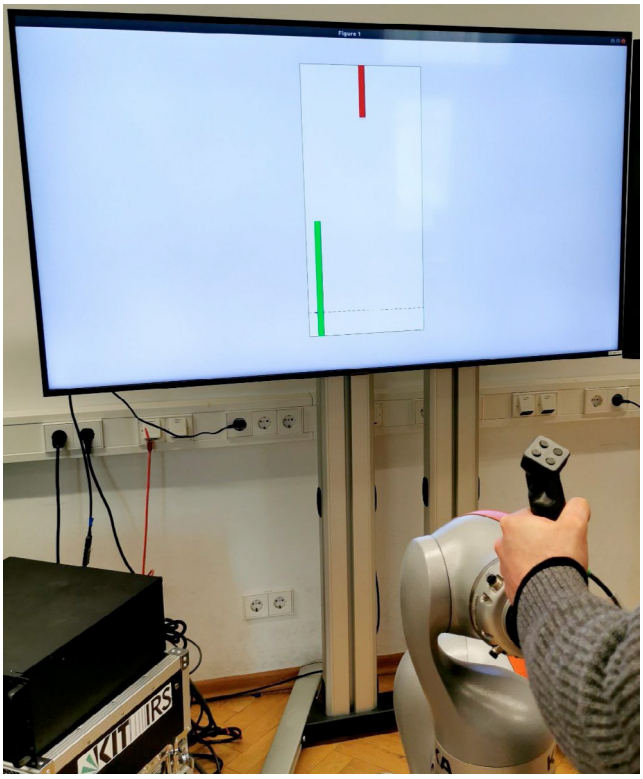

Fig. 2. Experimental setup. The haptic interface is displayed in the foreground, allowing a user to exert forces and receive haptic feedback on the position. The graphical user interface is depicted in the background. It displays the current simulated mass position as a cross, a reached reference position in green and an approaching reference position in red.

$$J_\mathrm{H} = \mathrm{E}\Bigg\{ \boldsymbol{x}_N^\intercal \boldsymbol{Q}_{\mathrm{H},N} \boldsymbol{x}_N + \sum_{t=0}^{N-1} \left(\boldsymbol{x}_t^\intercal \boldsymbol{Q}_{\mathrm{H},t} \boldsymbol{x}_t + \boldsymbol{u}_{\mathrm{H},t}^\intercal \boldsymbol{R}_\mathrm{H} \boldsymbol{u}_{\mathrm{H},t} \right) \Bigg\}, \tag{3}$$

with $\boldsymbol{Q}_{\mathrm{H},t} \in \mathbb{R}^{n \times n}$ being symmetric and positiv semidefinite for $t = 0, ..., N-1$ and $\boldsymbol{R}_\mathrm{H} \in \mathbb{R}^{m \times m}$ being symmetric and positive definite. We can transform (3) into a form that allows penalizing a deviation from a reference state (i.e. $\boldsymbol{x}_t - \boldsymbol{x}_\mathrm{ref}$) by introducing additional position states $\boldsymbol{p}_\mathrm{ref}$ with constant dynamics, see e.g. Todorov and Jordan (2002), thus enabling the analyzis of point-to-point movements from one point $\boldsymbol{T}_i = \boldsymbol{p}_{\mathrm{ref},i}$ to the next point $\boldsymbol{T}_{i+1} = \boldsymbol{p}_{\mathrm{ref},i+1}$.

An approximate solution to this optimal control problem can be found with

$$\begin{aligned} \boldsymbol{u}_{\mathrm{H},t} &= -\boldsymbol{L}_{\mathrm{H},t} \hat{\boldsymbol{x}}_{\mathrm{H},t}, \\ \hat{\boldsymbol{x}}_{\mathrm{H},t+1} &= \boldsymbol{A} \hat{\boldsymbol{x}}_{\mathrm{H},t} + \boldsymbol{B}_\mathrm{H} \boldsymbol{u}_{\mathrm{H},t} + \boldsymbol{K}_{\mathrm{H},t} \left(\boldsymbol{y}_{\mathrm{H},t} - \boldsymbol{H}_\mathrm{H} \hat{\boldsymbol{x}}_{\mathrm{H},t} \right), \end{aligned}$$

where $\hat{\boldsymbol{x}}_\mathrm{H}$ denotes the estimated system state by the human. For a detailed derivation we refer to Todorov (2005) and Karg et al. (2024).

2.4 Inverse Stochastic Optimal Control

To derive a control law that respects human variability, a proper knowledge of the natural human behavior is needed. Therefore the cost function matrices $\boldsymbol{Q}_{\mathrm{H},N}, \boldsymbol{Q}_\mathrm{H}, \boldsymbol{R}_\mathrm{H}$ and noise scaling parameters $\boldsymbol{\Sigma}^{\boldsymbol{\alpha}}, \boldsymbol{\sigma}_i^{\boldsymbol{u}}, \boldsymbol{\Sigma}^{\boldsymbol{\beta}}$, $\boldsymbol{\sigma}_i^{\boldsymbol{x}}$ need to be identified. We use the identification algorithm presented by Karg et al. (2024). It allows the identification of the above parameters, based on a set of time-discrete measured system trajectories $\boldsymbol{M}\boldsymbol{x}_t^{*,(k)}$, with $\boldsymbol{x}_t^{*,(k)}$ being one repetition of the stochastic process $\boldsymbol{x}_t^*$ which results from the closed-loop LQS system. The unknown parameters that result in the observed trajectories are represented by $\boldsymbol{s}^*$ and $\boldsymbol{\sigma}^*$, which combine the cost function parameters and the noise scaling parameters, respectively. $\boldsymbol{M}$ reduces the full system state to only the observable system states. For a detailed explanation of the algorithm we refer to their publication.

3. SUBJECT STUDY

Our experimental system as well as the study procedure is introduced in this section.

3.1 Experimental System

For our present experiments, we choose a simulated mass-damper system which shows a close analogy to related works in neuroscience and works analyzing pHRI. The former represent the human hand as a point mass, the latter analyze e.g. the collaborative manipulation of a

tool. The following dynamic equations for the x-dimension result:

$$p_{x,t+1} = p_{x,t} + \Delta t\, \dot{p}_{x,t}, \tag{4a}$$

$$\dot{p}_{x,t+1} = \left(1 - \Delta t \frac{d}{m}\right) \dot{p}_{x,t} + \frac{\Delta t}{m} f_{x,t}, \tag{4b}$$

with p_x and $\dot{p}_x$ denoting the position and velocity of the point mass m with the damping factor d. Furthermore we define the human muscle force $f_{x,t}$ to be the output of a second-order linear filter g_x with the human neural activation $u_{\mathrm{H},x}$ as input:

$$f_{x,t+1} = \left(1 - \frac{\Delta t}{\tau_2}\right) f_{x,t} + \frac{\Delta t}{\tau_2} g_{x,t} + u_{\mathrm{A},x,t}, \tag{5a}$$

$$g_{x,t+1} = \left(1 - \frac{\Delta t}{\tau_1}\right) g_{x,t} + \frac{\Delta t}{\tau_1} u_{\mathrm{H},x,t}. \tag{5b}$$

An automation's input $u_{\mathrm{A},x}$ would add to the overall exerted force f_x. The system state is defined as $\boldsymbol{x} = [p_x\ \dot{p}_x\ f_x\ g_x\ p_{x,\mathrm{ref}}]^\intercal$. The manipulated object is simulated as a point-mass with an inertia of $m = 50\,\mathrm{kg}$ and damped with $d = 75\,\mathrm{kg/s}$. We constraint the system to be movable in the x-dimension only. From the dynamic equations, the human system matrices $\boldsymbol{A}$ and $\boldsymbol{B}_\mathrm{H}$ can be derived. Regarding the human perception, we set $\boldsymbol{H}_\mathrm{H} = [\boldsymbol{I}_{3\times3}\ \boldsymbol{0}_{3\times2}]$.

We model independent stochastic processes $\boldsymbol{\alpha}$ and $\boldsymbol{\beta}$ for each state and output: $\boldsymbol{\Sigma}^{\boldsymbol{\alpha}} = \mathrm{diag}([\sigma_1\ \sigma_2\ \sigma_3\ \sigma_4\ 0])$ and $\boldsymbol{\Sigma}^{\boldsymbol{\beta}} = \mathrm{diag}([\sigma_5\ \sigma_6\ \sigma_7])$. For the signal-dependend noise processes we define:

$$\begin{aligned}
\sigma^u \boldsymbol{B}_\mathrm{H}\boldsymbol{F} &= \sigma_8 \boldsymbol{B}_\mathrm{H},\\
\sigma_1^x \boldsymbol{H}_\mathrm{H}\boldsymbol{G}_1 &= \sigma_9 \boldsymbol{H}_\mathrm{H}\mathrm{diag}([1\ 0\ 0\ 0\ 0]),\\
\sigma_2^x \boldsymbol{H}_\mathrm{H}\boldsymbol{G}_2 &= \sigma_{10} \boldsymbol{H}_\mathrm{H}\mathrm{diag}([0\ 1\ 0\ 0\ 0]),\\
\sigma_3^x \boldsymbol{H}_\mathrm{H}\boldsymbol{G}_3 &= \sigma_{11} \boldsymbol{H}_\mathrm{H}\mathrm{diag}([0\ 0\ 0\ 0\ 1]).
\end{aligned}$$

3.2 Procedure

In the study, 13 participants with a mean age of 24.5 ± 4.2 took part. All subjects are right-handed and male. First, the subjects get to familiarize themselves with the system through a test run of 45 s. During the main part of the study, the subjects are instructed to perform a 1-dimensional reaching task, moving a virtual mass between reference points which are located at $T_x = -12\,\mathrm{cm}/0\,\mathrm{cm}/12\,\mathrm{cm}$ on the x-axis. The 75 reference blocks appear pseudorandomized at the top of the screen and move downwards where they are to be held for 3.4 s. Short movements of 12 cm to and from $T_x = 0\,\mathrm{cm}$ are to be performed within 2.6 s, long movements of 24 cm within 4.1 s. A successful reaching of a reference point is indicated by tbe reference block turning from red to green. The main study part takes 9 mins. We focus on identifying the long movement from $T_x = -12\,\mathrm{cm}$ to $T_x = 12\,\mathrm{cm}$, which was repeated 20 times.

4. RESULTS & DISCUSSION

This subsection first presents how the data analysis was approached, before presenting the gained results from our subject study and discussing them.

4.1 Analysis

For data processing, the system position p_x is approximated using a cubic spline. The velocity is then calculated using numerical differentiation. Position and velocity formulate the observed system states that are used for the identification procedure. For each movement repetition, we determine the starting time as the last point where $|v|$ is approx. 0 m/s. Repetitions which do not fall below that threshold are removed from the dataset. We then calculate the average human behavior $\boldsymbol{x}_t^*$ and variance $\boldsymbol{\Omega}_t^{\boldsymbol{x}^*}$ based on all repetitions of one type of movement by one subject.

In order to identify the cost function and noise parameters of the human, we use the inverse stochastic optimal control algorithm introduced by Karg et al. (2024). The measured data is sampled with 100 Hz, however we downsample to 25 Hz for easier handling the data. This results in 110 time steps and 4.4 s for the analysed movement.

4.2 Results

Firstly, we analyze the measured data. Figure 3a displays the mean and covariance of the position and velocity data of each subject, moving from $-12\,\mathrm{cm}$ to $T_x = 12\,\mathrm{cm}$. Looking at the mean position, all subjects are able to reach the goal point within the specified time with a maximum position error of 5%. The velocity profiles match the expected point-to-point reaching features: They are single-peaked and mostly bell-shaped and symmetric. All profiles are slightly left-skewed. Subject 11 shows a strong outlier behavior, exhibiting a much higher mean velocity. This results in an earlier average reaching of the target point, but comes with a much higher variance in position and velocity compared to the other subjects.

The covariance data also matches the expected features: the position variance profiles are bell-shaped, single peaked and mostly symmetric. They all reach values close to zero, with the variance at $t = 5\,\mathrm{s}$ always being smaller than $5 \times 10^{-5}\,\mathrm{m}^2$. The peak values in position variance differ greatly between the subjects, with the smallest peak variance reaching $2 \times 10^{-4}\,\mathrm{m}^2$ and largest peak variance being at $9.5 \times 10^{-4}\,\mathrm{m}^2$, excluding the outlier S11. The velocity variance profiles show two peaks and, except for outlier S11, are symmetric and display a visible decrease in variance between the two peaks.

For the identification, we take the average behavior over all subjects except the outlier subject S11. Figure 3b shows the mean measured data as well as the LQS model predictions for the average and variance of position and velocity. Looking at the model predictions qualitatively, the LQS model prediction profiles match with the measured data: single-peaked position variance and single peaked mean velocity profiles, as well as double-peaked velocity variance. The absolute value of the modeled velocity peak matches the measured data, however, the modeled behavior displays a delayed response compared to the measured data which also shows in the delayed position curve. Regarding the position variance, the peak covariance value is predicted with an error of 19% to the maximum value and does not flatten towards the end of the movement as much as observed in the measured data. Looking at the velocity variance, the douple-peaked shape of the measured data

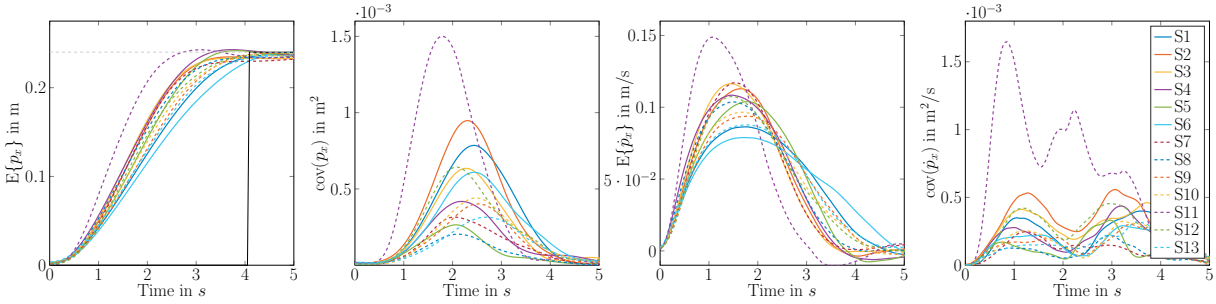

(a) Mean and variance of the measured data for each subject.

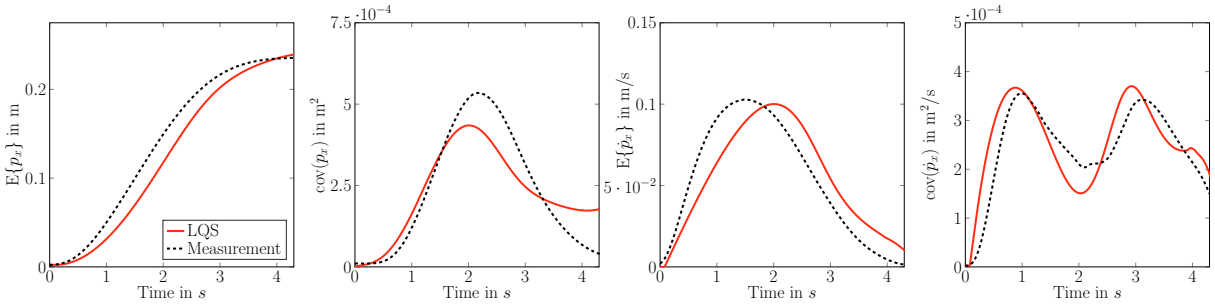

(b) Mean measured data and LQS model prediction over all subjects except outlier subject S11.

is predicted accordingly. Predicted peak variance values show errors of 3% and 8% and the predicted variance at the end of the movement shows an error of 16%.

4.3 Discussion

The goal of this paper is the identification of human natural variability behavior in a real reaching task. This aims at providing a basis for controller development which explicitly considers this variability in the control design and parametrization. Therefore, especially the qualitative shape and key values of the predicted model are of interest. The results show that the used identification procedure suits our goal: Since the shape and the magnitude of values of the predictions matches the measured data, the presented results can be used as a basis for variability-respecting controller designs. Merely the predicted position variance peak does not perfectly match with the observed data. With an error of less than 20% however, the predicted magnitude and overall shape can still be used as a basis for personalization.

Whether the identified mean behavior over all subjects or an individual identification could lead to improved performance and perception needs to be analyzed in further works. The large spread in position variance peak values indicates that an individual identification or an identification by subgroups will be needed, instead of an identification over all subjects. This however shows, that human behavior is individual and an identification of human noise processes might be beneficial for human-centered control design.

5. CONCLUSION & OUTLOOK

In this paper we present an experimental system setup that allows a human to interact with a simulated system which emulates the position manipulation of a large tool. On this system, a subject study examining point-to-point reaching movements with 13 participants is performed. Based on the measured data, a LQS model of human movement behavior, including stochastic noise processes, is identified using an inverse stochastic optimal control approach. Both the qualitative shape and magnitude of the predicted behavior matches the measured data. This provides a crucial basis for further work, which can use the identified data to design more human-centered control designs. In the next steps, identified models which predict either individual or sub-group behavior can be used to parametrize control concepts that explicitly consider a subjects individual variability.

REFERENCES

Abbink, D.A., Mulder, M., and Boer, E.R. (2012). Haptic shared control: Smoothly shifting control authority? *Cognition, Technology & Work*, 14(1), 19–28. doi: 10.1007/s10111-011-0192-5.

Abend, W., Bizzi, E., and Morasso, P. (1982). Human Arm Trajectory Formation. *Brain*, (105), 331–348. doi: 10.1093/brain/105.2.331.

Berret, B., Chiovetto, E., Nori, F., and Pozzo, T. (2011). Evidence for Composite Cost Functions in Arm Movement Planning: An Inverse Optimal Control Approach. *PLoS Computational Biology*, 7(10), e1002183. doi: 10.1371/journal.pcbi.1002183.

Braun, C.A., Haide, L., Fischer, L., Kille, S., Varga, B., Rothfuss, S., and Hohmann, S. (2023). Using a Collaborative Robotic Arm as Human-Machine Interface: System Setup and Application to Pose Control Tasks. In *2023 IEEE International Conference on Robotics and Automation (ICRA)*, 12464–12470. IEEE. doi: 10.1109/ICRA48891.2023.10161348.

Chen, X. and Ziebart, B. (2015). Predictive Inverse Optimal Control for Linear-Quadratic-Gaussian Systems. In *Proceedings of the Eighteenth International Conference on Artificial Intelligence and Statistics*, 165–173. PMLR.

Dong, J., Xu, J., Zhou, Q., and Hu, S. (2020). Physical human–robot interaction force control method based on adaptive variable impedance. *Journ. of the Franklin Institute*, 357(12), 7864–7878. doi: 10.1016/j.jfranklin.2020.06.007.

Ficuciello, F., Villani, L., and Siciliano, B. (2015). Variable Impedance Control of Redundant Manipulators for Intuitive Human–Robot Physical Interaction. *IEEE Trans. on Robot.*, 31(4), 850–863. doi: 10.1109/TRO.2015.2430053.

Franceschi, P., Beschi, M., Pedrocchi, N., and Valente, A. (2023). Modeling and Analysis of pHRI with Differential Game Theory. In *21st Int. Conf. on Advanced Robotics (ICAR)*, 277–284. doi: 10.1109/ICAR58858.2023.10406758.

Guerin, K.R., Riedel, S.D., Bohren, J., and Hager, G.D. (2014). Adjutant: A framework for flexible human-machine collaborative systems. In *2014 IEEE/RSJ International Conference on Intelligent Robots and Systems*, 1392–1399. IEEE.

Harris, C.M. and Wolpert, D.M. (1998). Signal-dependent noise determines motor planning. *Nature*, 394(6695), 780–784. doi:10.1038/29528.

Karg, P., Hess, M., Varga, B., and Hohmann, S. (2024). Bi-Level-Based Inverse Stochastic Optimal Control. In *2024 European Control Conference (ECC)*, 537–544. doi:10.23919/ECC64448.2024.10591104.

Karg, P., Stoll, S., Rothfuß, S., and Hohmann, S. (2023). Validation of Stochastic Optimal Control Models for Goal-Directed Human Movements on the Example of Human Driving Behavior. *IFAC-PapersOnLine*, 56(2), 8320–8326. doi:10.1016/j.ifacol.2023.10.1021.

Kille, S., Leibold, P., Karg, P., Varga, B., and Hohmann, S. (2024). Human-Variability-Respecting Optimal Control for Physical Human-Machine Interaction. In *IEEE RO-MAN 2024*. Pasadena, USA.

Liu, C.K., Hertzmann, A., and Popovic, Z. (2005). Learning physics-based motion style with nonlinear inverse optimization. *ACM Transactions on Graphics*, 24(3). doi:10.1145/1073204.1073314.

Mombaur, K., Truong, A., and Laumond, J.P. (2010). From human to humanoid locomotion—an inverse optimal control approach. *Autonomous Robots*, 28(3), 369–383. doi:10.1007/s10514-009-9170-7.

Mulder, M., Abbink, D.A., and Boer, E.R. (2012). Sharing Control With Haptics: Seamless Driver Support From Manual to Automatic Control. *Human Factors: The Journal of the Human Factors and Ergonomics Society*, 54(5), 786–798. doi:10.1177/0018720812443984.

Panchea, A.M., Ramdani, N., Bonnet, V., and Fraisse, P. (2018). Human Arm Motion Analysis Based on the Inverse Optimization Approach. In *7th IEEE Int. Conf. on Biomedical Robotics and Biomechatronics (BioRob)*, 1005–1010. IEEE. doi:10.1109/BIOROB.2018.8488045.

Priess, M.C., Choi, J., and Radcliffe, C. (2014). The Inverse Problem of Continuous-Time Linear Quadratic Gaussian Control With Application to Biological Systems Analysis. In *ASME 2014 Dynamic Systems and Control Conference*. American Society of Mechanical Engineers Digital Collection. doi:10.1115/DSCC2014-6100.

Quigley, M., Conley, K., Gerkey, B., Faust, J., Foote, T., Leibs, J., Wheeler, R., and Ng, A.Y. (2009). ROS: An open-source Robot Operating System. In *ICRA Workshop on Open Source Software*, volume 3, 5. Kobe, Japan.

Rothfuß, S., Inga, J., Köpf, F., Flad, M., and Hohmann, S. (2017). Inverse Optimal Control for Identification in Non-Cooperative Differential Games. *IFAC-PapersOnLine*.

Schneider, J., Rothfuß, S., and Hohmann, S. (2022). Negotiation-based cooperative planning of local trajectories. *Frontiers in Control Engineering*, 3, 1058980.

Sylla, N., Bonnet, V., Venture, G., Armande, N., and Fraisse, P. (2014). Human arm optimal motion analysis in industrial screwing task. In *5th IEEE RAS & EMBS Int. Conf. on Biomedical Robotics and Biomechatronics (BioRob)*, 964–969. doi: 10.1109/BIOROB.2014.6913905.

Todorov, E. (2005). Stochastic Optimal Control and Estimation Methods Adapted to the Noise Characteristics of the Sensorimotor System. *Neural Comput.*, (17), 1084–1108.

Todorov, E. and Jordan, M.I. (2002). Optimal feedback control as a theory of motor coordination. *Nat. Neurosci.*, 5(11), 1226–1235. doi:10.1038/nn963.

Varga, B. (2024). Toward Adaptive Cooperation: Model-Based Shared Control Using LQ-Differential Games. *Acta Polytechnica Hungarica 2024*, 21(10), 439–456. doi: 10.12700/APH.21.10.2024.10.27.

Wang, Q., Cheng, Y., Jiao, W., Johnson, M.T., and Zhang, Y. (2019). Virtual reality human-robot collaborative welding: A case study of weaving gas tungsten arc welding. *Journal of Manufacturing Processes*, 48, 210–217.